ABSTRACT

Title of Document: LOW DIMENSIONAL DESCRIPTION OF PEDESTRIAN-INDUCED INSTABILITY OF THE MILLENNIUM BRIDGE

Mahmoud M. Gad Abdulrehem, Master of Science, 2008

Directed By: Professor Edward Ott,
Electrical and Computer Engineering Department

When it opened to pedestrian traffic in the year 2000, London's Millennium Bridge exhibited an unwanted, large, side-to-side oscillation which was apparently due to a resonance between the stepping frequency of walkers and one of the bridge modes. Models for this event, and similar events on other bridges, have been proposed. The model most directly addressing the synchronization mechanism of individual walkers and the resulting global response of the bridge-pedestrian system is one developed by Eckhardt *et al*. This model treats individual walkers with a phase oscillator description and is inherently high dimensional with system dimensionality ($N+2$), where N is the number of walkers.

In this thesis we use a method proposed by Ott and Antonsen to reduce the Eckhardt *et al*. model to a low dimensional dynamical system, and we employ this reduced description to study the global dynamics of the bridge-pedestrian interaction. More generally, this treatment serves as an interesting example of the possibility of low dimensional macroscopic behavior in large systems of coupled oscillators.

LOW DIMENSIONAL DESCRIPTION OF PEDESTRIAN-INDUCED INSTABILITY OF THE MILLENNIUM BRIDGE

By

Mahmoud M. Gad Abdulrehem

Thesis submitted to the Faculty of the Graduate School of the
University of Maryland, College Park, in partial fulfillment
of the requirements for the degree of
Master of Science
2008

Advisory Committee:
Professor Edward Ott, Chair/Advisor
Professor Amr Baz
Assistant Professor Michelle Girvan

Dedication

To my beloved wife, Mai, who offered me unconditional love and support.

Acknowledgements

I would like to express my deepest gratitude to Professor Edward Ott for his generosity in offering me help, support and encouragement throughout the writing of this dissertation. His meticulous supervision has not only educated in me research work but it will also be an inspiration and a model to follow in the future. Without his guidance and support, this dissertation would not have been possible.

My special thanks go to my parent and family without whose support and help I would not have made it.

Last but not least, I would like to thank my dear wife, Mai ElAmir, for the unlimited support and help she has given me through the occasional hard times and moments of frustration that often happen during research work. Without her advice and moral support, my task and life here in College Park would have been infinitely harder.

Table of Contents

List of Tables

List of Figures

Chapter 1: Introduction

In recent decades there has been a trend towards improved mechanical characteristics of materials used in footbridge construction. This has enabled engineers to design lighter, more slender and more aesthetic structures. As a result of these construction trends, many footbridges have become more susceptible to vibrations when subjected to dynamic loads.

One of the most recent examples is the Millennium Bridge in London. As an eager crowd streamed onto the bridge for the opening celebration, the bridge developed large amplitude side-to-side oscillations, and the crowd simultaneously began to fall into step.

Some models were developed to understand this phenomenon. The most recent one is by Eckhardt *et al.* [3]. It models the bridge and the pedestrian movement as a coupled oscillator system. This model gives substantial insight about the problem and what happened on the opening day. The limitation of this model is that it is difficult to track analytically.

In this work, we study the dynamics of the model from Ref. [3] by employing a technique developed in Ref. [18] that allows us to provide an exact reduction of the original high dimensional dynamical system to a low dimension description. This low dimensional model enables us to study the bridge instability analytically and, in addition, greatly facilitates the numerical investigation.

1.1 Thesis Navigation

In chapter 2 we introduce the Millennium Bridge stability problem including a brief description of measurements and tests performed by the company (Arup) that designed the bridge.

In chapter 3 we review existing models for the Millennium Bridge problem and their limitations.

In chapter 4, we analytically reduce the model of Ref. [3] to an equivalent lower dimensional model, and we present analysis of our reduced model.

Numerical simulation results are presented in chapter 5, along with a comparison between our results and Arup's measurements.

Finally, we present conclusions and further discussion in chapter 6.

Chapter 2: The Story of the Millennium Bridge

2.1 Introduction

The London Millennium Footbridge is a pedestrian steel suspension bridge crossing the River Thames in London, England, linking Bankside with the City. The southern end of the bridge is near the Globe Theatre, the Bankside Gallery and Tate Modern, the north end is next to the City of London School below St Paul's Cathedral. The bridge alignment is such that a clear view of St Paul's south facade is presented from across the river, framed by the bridge supports, thus providing a scenic view of the cathedral, see Fig. 2.1.

Figure 2.1: The Millennium Bridge with St. Paul's Cathedral on the left [4].

2.2 The Opening Day

On opening day and as an eager crowd streamed onto the bridge for the opening celebration, pedestrians experienced a large lateral wobbling of the bridge. The wobbling increased as more and more people streamed onto the bridge. This phenomenon apparently was due to a resonance between a low order bridge mode and the natural average stepping frequency of human walkers.

City authorities closed the bridge two days after its opening. During the following 18 months, the designer company, Arup, developed a system of dampers aimed at eliminating the unwanted wobble. In the next sections we will review Arup's measurements and solution.

2.3 Arup's Controlled Tests

After the bridge was closed, Arup initiated a series of experiments to better determine the number of pedestrians necessary to destabilize a given span of the bridge. These tests were administered by having Arup employees enter the north span in a controlled fashion, so that the size of the crowd was known, while accelerometers recorded the resulting vibrations. Further walkers were added to the span in groups.

The solid plot in Fig. 2.2 shows the time evolution of the bridge vibration versus time. The dashed line is the number of people walking on the bridge. This starts with around 50 walkers, further walkers are added to the span in groups of around 10 people.

Arup's engineers concluded from this experiment that, the north span is stable with 156 people but with just 10 more people the movements increase suddenly and synchronous lateral excitation occurred. More details on the correctness of these conclusions will be discussed in chapter 3 and chapter 5.

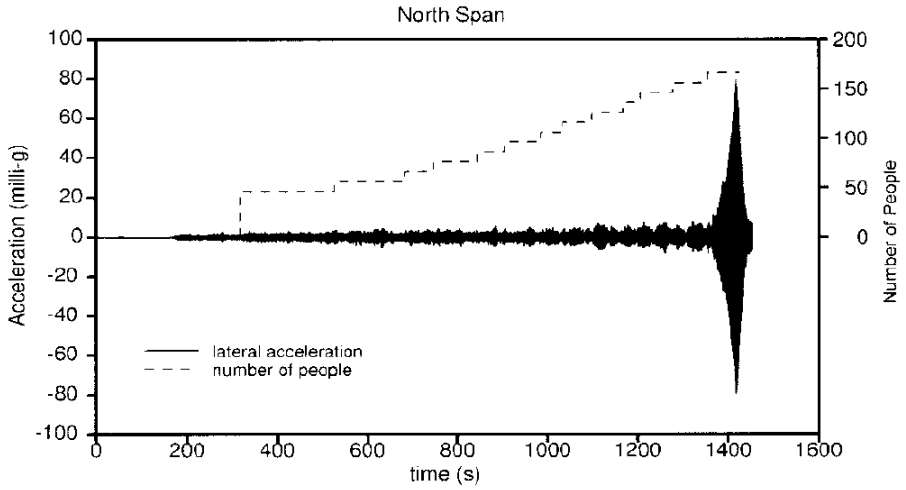

Figure 2.2: A time trace of lateral acceleration of the bridge deck and the number of pedestrians (taken from Arup's measurements [5]).

2.4 Arup's Solution

There are two fundamental ways to limit dynamic excitation. The first is to stiffen the structure, so the natural lateral oscillation frequency of the bridge becomes very different from the stepping frequency of pedestrians. The second is to add damping to absorb the energy of lateral oscillation.

Arup concluded that stiffening the bridge to change its frequency was not a feasible option. The bridge would need to be at least tenfold stiffer laterally to move its frequency out of the excitation range, and the additional structure required to do this would dramatically change the appearance of the bridge.

It was decided to adopt a damping solution, either active damping or passive damping. Active damping uses powered devices to apply forces to the structure to counteract vibrations. Passive damping relies on harnessing the movements of the structure to absorb energy.

Active dampers are commonly used in other engineering fields such as aeronautics and buildings. However, no previously designed systems were sufficiently developed for a more complex multimodal system such as the bridge. Maintenance requirements were also a cause for concern. Following discussions with manufacturers, Arup reached the conclusion that active damping was too complex and expensive and that production times were too long for this to be a viable solution in this instance.

The bridge deploys passive damping to reduce bridge movement. Figure 2.3 shows a passive viscous damper that was employed to reduce lateral motion.

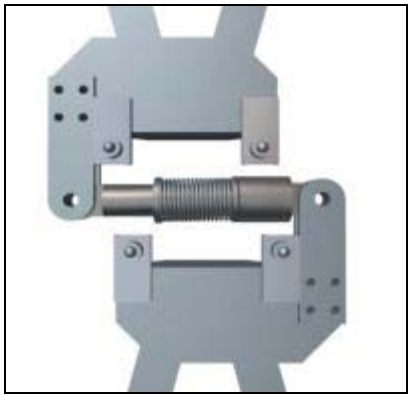

Figure 2.3: Illustration of a viscous damper implemented in the Millennium Bridge.

These Viscous dampers are located under the deck, around the piers and the south landing to control the lateral motions. They function in a similar way to shock absorbers. Each damper dissipates energy by the movement of a piston passing back and forth through a fluid. Distinctive new chevron steelwork transfers the bridge movements to the under deck viscous dampers.

In addition to viscous dampers used to damp lateral motion, tuned mass dampers are also located beneath the deck and reduce vertical movements. Tuned to a specific frequency these inertial devices, simplistically weights on springs, are attached to discrete points on the structure. Although no excessive vertical movement occurred on the Millennium Bridge, these were added as a precaution, since some researchers suggested that synchronous pedestrian vertical loading is also possible and has been observed elsewhere. Figure 2.4 shows the positions where dampers were added to the bridge.

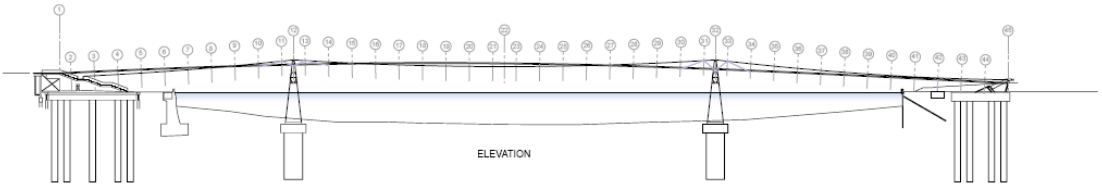

Figure 2.4: Elevation of the bridge showing the dampers' positions [4].

2.5 Other Bridges

The Millennium Bridge oscillation is different from that which lead to the destruction of the Tacoma Narrows Bridge. In particular, for the Millennium Bridge there is no mechanical bridge resonance near the frequency of vortex shedding induced by wind nor are there vibrations of the empty bridge both of which occurred

in the case of the Tacoma Bridge. There was no swaying with few moving people or with people standing still. The Millennium Bridge oscillation happened when the number of moving pedestrian crossed a critical number.

It appears that little in the way of lateral phenomena has been previously recorded for other footbridges. A documented case is that of a footbridge in Japan connecting a sports facility to a bus terminal. The bridge suffered strong lateral motions when crowds crossed it at the end of an event [7]

More recently, lateral vibrations were among several reasons behind the closure of the new Solferino Bridge in Paris, Fig. 2.5, immediately after its opening in December 1999. The 100 year-old Alexandra Bridge in Ottawa, Fig. 2.6, experienced strong lateral vibrations in July 2000, when subjected to abnormal crowd loading, in this case by spectators of a fireworks display.

Figure 2.5: Pont du Solferino, Paris, France

Figure 2.6: Alexandra Bridge, Ottawa, Canada

2.6 Bridge Parameters

The data relevant to opening day is limited to some archival video footage. Peak crowd densities can be estimated from the videos and from published Arup statistics at about 1.3-1.5 persons per square meter, or about 450 total walkers on the north span [4, 5].

Because the majority of published experimental data pertains to the fundamental lateral mode of the north span, we have used those parameters in most of the calculations presented in the following chapters. Table 2.1 presents a summary of the published data for the three spans of the Millennium Bridge.

Table 2.1: Millennium Bridge parameters for the fundamental lateral mode on the north span, center span, and south span. Data comes from [4, 5]. The 'damping ratio' in this table is the same as what we define as $\tilde{\varepsilon}$ in Sec. 4.2

	North span	Central span	South span
Length [m]	81	144	108
Modal mass [kg x 103]	113	128-130	160
Resonant frequency [Hz]	1.03	0.48	0.80
Damping Ratio [%]	0.6-0.8	0.765	0.6-0.8

The resonant frequencies of various footbridges are presented for comparison in Fig. 2.7 (from [5]). It is interesting to note that a substantial number of these footbridges have resonance in the dangerous region near 1 Hz.

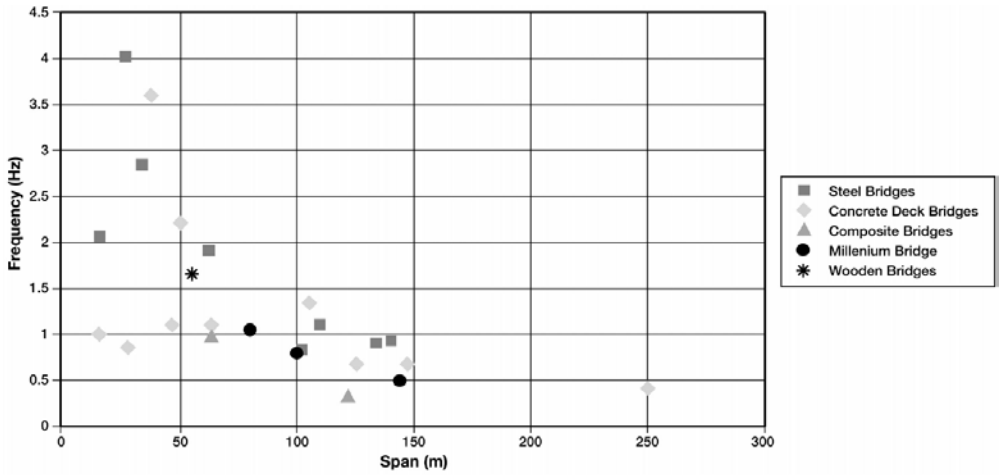

Figure 2.7: Natural frequencies of footbridge spans of varying lengths composed of different materials. (Taken from [5]).

Chapter 3: Millennium Bridge Models

In this section, we review existing theories of the lateral vibration on the Millennium Bridge.

3.1 Arup's Model

Arup engineers published a series of papers [4, 5, 6] in which they describe the experiments they carried out and the theory that they developed to explain the onset of lateral oscillation

The key modeling assumption of this work is that pedestrians act like negative damping. Thus they formulate a model, where the correlated lateral force per person F is proportional to the local lateral bridge velocity V, i.e., $F = kV$. The proportionality constant k was measured empirically to be about 300 kg/s (see Fig. 3.1). The lateral correlated force was estimated in experiment by measuring the gain in kinetic energy per cycle, under the assumption that the work done must have come from the difference between pedestrian forcing and known damping.

Arup found a formula for the critical number of pedestrians by solving for the point at which the bridge damping is exactly counteracted by pedestrians' effective negative damping.

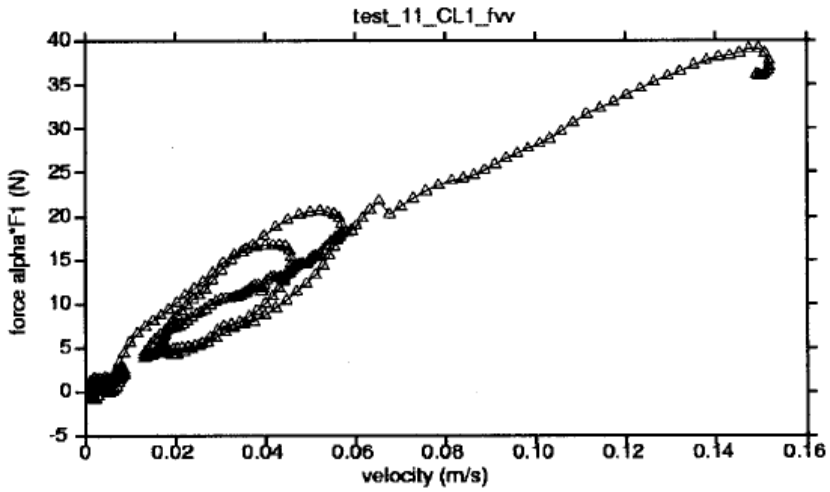

Figure 3.1: Typical lateral force versus velocity. Experimental results based on Arup's controlled tests conducted after closure of the Millennium Bridge [5].

The primary disadvantage of Arup's model is the empirical nature of the description of pedestrians. The linear relationship between F and V, if indeed correct, should be explained by the model, rather than assumed.

Also, the empirical law does not address *why* pedestrians act like a negative damping, nor address the issue of pedestrian walking synchronization. Video footage from opening day clearly shows that pedestrian stepping synchronization occurred and was related to the unwanted wobble.

Another downside to this approach is that the predicted critical number of pedestrians depends only on the damping, and is independent of the natural frequency of the bridge. Different bridges have different critical thresholds. The crucial effect of the walker frequency distribution is also not considered in this model

Finally, the steady state amplitude for bridge motion cannot be predicted, as it is due to nonlinearities that are not modeled in Arup's system

3.2 Newland's Model

In 2003, Newland published a two parts paper relating to the Millennium Bridge problem [16].

In his first part he defined a transfer function for the effect of forces on the bridge and another for the feedback on the people. He then assumes, based on the empirical evidence of Arup's tests, that the pedestrians naturally tend to shift their phases such that they maximally destabilize the bridge (a worst-case scenario). By solving for the phase in the feedback transfer function at which the bridge is maximally destabilized, he claims to show that pedestrians do indeed act like negative dampers (i.e., their force leads bridge displacement by $\pi/2$ in phase) under such assumptions

In the second part, he explores the problem with the approach of a delayed differential equation, assuming that pedestrian motion $z(t)$ is smaller in amplitude than the bridge motion $y(t)$ and delayed by a value Δ, i.e., $z(t) = \alpha y(t - \Delta)$ where α is positive. A steady oscillatory state assumption $y(t) = Y e^{i\omega t}$ results in a stability condition for the bridge damping. It is assumed that only some fraction β of the population locks into synchronization with the bridge. Both β and α are estimated from Arup's experimental data and found to be $\alpha \approx 2/3$ and $\beta \approx 0.4$.

The model assumes that 40% of the walkers are locked to the bridge frequency regardless of that natural frequency and regardless of the amplitude of motion. The model does not account for differences in walker frequency distributions, and does not address the question of steady-state amplitude of bridge motion.

3.3 Roberts' Model

In the 2003 paper Ref. [19] by Roberts, the bridge was modeled using partial differential equations. The pedestrians were assumed to have a sideway acceleration proportional to the interaction force, which is assumed sinusoidal with a frequency different from the bridge eigenfrequencies.

The model assumes that pedestrians will synchronize so as to destabilize the bridge; it does not describe the underlying cause of the synchronization. Because of that, it cannot describe the onset of the synchronization/vibration, and therefore cannot explain Arup's empirical law for linearity between pedestrian forcing and bridge velocity.

3.4 Nakamura's Model

Nakamura's work [15] starts from the model by Arup, but includes the additional assumption that a pedestrian response to bridge motion will saturate at large amplitudes. That is, he assumes that Arup's $F = kV$ is only valid for small bridge velocities.

Nakamura's predictions match those of Arup for onset of the instability. The difference in his work is that the steady state amplitude may be predicted, although no algebraic solution is given, only numerical results are presented.

Synchronization is assumed but not explained, and the critical number of pedestrians, implicit in Nakamura's model, is independent of the natural frequency of the bridge.

3.5 Fujino's Model

Motivated by an earlier observation of wobbling on a footbridge in Japan, the 1994 paper of Fujino *et al.* [7] start by modeling the bridge as a damped harmonic oscillator, driven sinusoidally by a crowd of identical walkers whose phases are initially randomly distributed. The implied predictions for steady-state amplitude are too small, so the authors review movie footage of a case of synchronous lateral excitation, and find that approximately 20% of the crowd is phase-synchronized. Using that assumption, they modify their predictions and find that the steady-state amplitudes in their model with 20% synchronization are reasonable

Fujino *et al.* predict that about 20% of the walkers on a laterally vibrating bridge will synchronize in phase. The steady state amplitude that they predict comes from the steady state behavior of a sinusoidally driven damped harmonic oscillator.

The model proposed by Fujino *et al.* does not predict any sudden transition to a vibrating bridge state; rather it yields a continuous increase in the vibration amplitude as the number of walkers increases. This conflicts with Arup's experiments made on the Millennium Bridge

Also, Fujino's model uses the empirical value of 20% synchronization without providing a theoretical basis. It does not indicate what causes that partial synchronization to occur, or at what amplitude it begins to happen

3.6 Eckhardt's Model

Eckhardt *et al*. [3] modeled the bridge lateral oscillation as a damped harmonic oscillator forced by the motion of the pedestrians,

$$M\ddot{y} + 2M\varepsilon\,\dot{y} + M\Omega^2 y = \sum_{i=1}^{N} f_i(t) \tag{3.1}$$

where $y(t)$ is the modal bridge displacement, Ω is the angular eigenfrequency associated with the relevant mode, M is the equivalent modal mass, ε is the damping rate, and the dots on y denote time derivatives. The lateral modal force exerted on the bridge by pedestrian i is $f_i(t)$, where i=1,2, . . . ,N, with N the number of pedestrians on the bridge.

In order to model the dynamics of the bridge-pedestrian system, the model attempts to incorporate the dynamics of the different responses of individual pedestrians as they adjust their stepping under the influence of the bridge motion.

A fundamental difficulty is that there does not currently exist a well-developed, generally accepted, physiological model of human walking dynamics and its response to external inputs [3].

The model considers the response of walkers to small bridge displacements, and assumes that the walker response is approximately linear in the bridge displacement. In addition, the following hypotheses are employed:

1. The effect results solely from an interaction between the bridge and the walkers and not from visual or other communication between the walkers, i.e., people-people interactions are not included in the model.

2. The only significant bridge variable sensed by the walkers is that due to the side-to-side force felt by the walkers in the moving frame of the bridge [i.e., the walkers directly sense only the side-to-side bridge acceleration, $\ddot{y}(t)$].

3. The dynamics of a walker's response to small amplitude bridge motion is describable within the phase oscillator framework,

$$\begin{aligned} f_i(t) &= f_{0_i} \cos\left(\theta_i(t)\right), \\ \dot{\theta}_i &= \omega_i - b\ddot{y}\cos\left(\theta_i(t)\right), \end{aligned} \tag{3.2}$$

where *b* is a coupling constant, f_{0_i} is the peak lateral force applied by the walker, and ω_i is the stepping frequency of walker *i*. (Note that a complete cycle consists of both left and right steps. More details on the walker frequency and force will be discussed in the next section).

3.7 Walker's Model

Modeling the pedestrian walking is harder than modeling the bridge response. First of all, very few studies have been done on the properties of pedestrians. One study [13, 14] has been done on pedestrians walking on a platform simulating the dynamics of a bridge. However, the pedestrian response dependency on the frequency of the forcing was not measured, and the phase relationship between the walker and the oscillating platform was not monitored.

3.7.1 Walkers Frequency

A statistical description of normal walking frequencies was first given by Matsumoto *et al*. [11, 12] who investigated a sample of 505 persons. They concluded that the frequencies approximately follow a normal distribution with a mean pacing rate of 2.0 Hz and standard deviation of 0.173 Hz. The result is shown in Fig. 3.2.

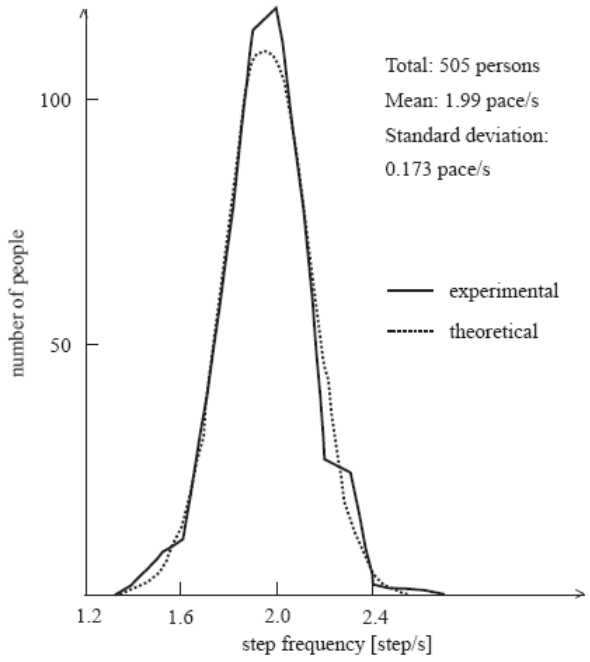

Fig 3.2: Distribution of pacing frequencies for normal walking (from [21]).

The book by Bachmann and Ammann [1] also discusses the loading from human motions, distinguishing between slow walking, walking, fast walking, jogging, and running. Table 3.1 shows the pacing frequency and the lateral frequency of each of the previous human motion types.

Table 3.1: Walking and running from Bachmann and Ammann [1]

	Pacing Frequency (Hz)	Lateral Frequency (Hz)
Slow walk	1.7	0.85
Normal walk	2.0	1.0
Fast walk	2.3	1.15
Slow running	2.5	1.25
Fast running	>3.2	>1.6

3.7.2 Walkers Force

Several statistical studies assess the pedestrian applies dynamic forces to the surface on which he/she walks. The variation in the vertical force component is estimated to be 40% of the walker's body weight. The lateral component is applied at half the footfall frequency and on a stationary surface is about 10% of the vertical component; i.e., 4% of body weight [2, 21].

Chapter 4: Low Dimensional Description of the Millennium Bridge Dynamics

In this chapter we will introduce a low dimension model for the Millennium Bridge problem. We start with a review of coupled oscillator system properties. Then a review of Eckhardt's *et al*. [3] model limitation is discussed. Then using the notion of order parameter, we will derive a low dimensional model for bridge stability. A detailed analysis of the bridge stability is carried out using this model.

4.1 Coupled Oscillators

Systems consisting of large number of coupled oscillators can be found in many significant applications. Examples are the synchronous flashing of groups of fireflies, coordination of oscillatory neurons governing circadian rhythms in animals [20], entrainment in coupled oscillatory chemically reacting cells [9], bubbly fluids [8], etc. A key contribution in this area was the introduction of the following model by Kuramoto [10],

$$\dot{\theta}_i = \omega_i + \frac{K}{N}\sum_{j=1}^{N}\sin\left(\theta_j(t) - \theta_i(t)\right) \tag{4.1}$$

where the state of oscillator *i* is given by its phase $\theta_i(t)$, $(i = 1, 2, \ldots\ldots, N)$, ω_i is the natural frequency of oscillator *i*, and the coupling constant *K* specifies the strength of the influence of one oscillator on another. It has been shown in Ref. [17] that in the $N \to \infty$ limit there is a continuous phase transition such that, for *K* below a critical value $(K < K_c)$, no coherent behavior of the system occurs (i.e., there is no global

correlation between the oscillator phases), while above the critical coupling strength $(K > K_c)$, the system displays continuously increasing global cooperative behavior (i.e., partial or complete synchronization of the phases).

The Millennium Bridge problem is somewhat more complicated than the situation envisioned for the applicability of Eq. (4.1), where the oscillators interact *directly* with coupling constant *K*. In contrast, the oscillators (walkers) in the Millennium Bridge problem interact through their mutual effect on a separate dynamical unit (the bridge). Nevertheless, these two models have in common their characterization of the oscillator state by a single simple scalar variable, $\theta_i(t)$.

4.2 Eckhardt's Normalized Model

In order to simplify the analysis, the model neglects the variation of the walker's weights. Hence we assume that $f_{0_i} = f_0$ for all *i*. This assumption could, without too much trouble, be lifted, i.e., the model framework could be easily generalized to include a distribution of the walker weights. However, we do not expect any important consequence due to a distribution of walker weights, and so will not attempt to include that complicating factor.

A dimensionless formulation of the model will be used through the rest of the chapter. Dimensionless quantities will be distinguished by a tilde over the corresponding symbols, as follows,

$$t = \tilde{t} / \Omega \tag{4.2}$$

$$y = \frac{N f_0}{M\Omega^2}\tilde{y} \tag{4.3}$$

$$\omega_i = \tilde{\omega}_i \Omega \tag{4.4}$$

$$\varepsilon = \tilde{\varepsilon}\Omega \tag{4.5}$$

and the normalized version of the model in Eqs. (3.1) and (3.2) becomes

$$\ddot{\tilde{y}} + 2\tilde{\varepsilon}\dot{\tilde{y}} + \tilde{y} = \frac{1}{N}\sum_{i=1}^{N}\cos\theta_i \tag{4.6}$$

$$\dot{\theta}_i = \tilde{\omega}_i - b\ddot{\tilde{y}}\cos\theta_i \tag{4.7}$$

where *b* is called the coupling coefficient and is given by

$$b = \frac{N f_0}{\Omega\tau M g_0}, \tag{4.8}$$

where g_0 and τ are constants defined in [3] characterizing the human walker response. The value of τ can be roughly estimated but has considerable uncertainty.

4.3 Eckhardt's Previous Work

Eckhardt, *et al*. in [3], developed the above-given bridge model, and they used it to understand the bridge oscillation phenomena. They assumed that the distribution of the walker's frequency is Gaussian

$$\tilde{g}\left(\tilde{\omega}\right) = \frac{1}{\sqrt{2\pi\sigma^2}} e^{\frac{-\left(\tilde{\omega}-\tilde{\omega}_0\right)^2}{2\sigma^2}} \tag{4.9}$$

for which they obtained extensive results.

For example, for $\tilde{\omega}_0 = 1$, analytical results were obtained for the critical number of people above which oscillation occurs,

$$N_c = 4\varepsilon M\Omega\left(\frac{2\tau g_0}{\pi\tilde{g}(1) f_0}\right) \tag{4.10}$$

where $\tilde{g}(1) = \left(\tilde{\sigma}\sqrt{2\pi}\right)^{-1}$.

In the next section we will introduce a solution of the problem based on the technique introduce in Ref. [18]. Using this technique we can analytically reduce the dimensionality of the ODE model (4.6) and (4.7) from (*N*+2) ODE's to 4 ODE's and we can analytically investigate the reduced system.

4.4 Bridge Instability Low Dimension Model

In this section we will use the technique of Ref. [18] to establish a lower order model of the Millennium Bridge problem. Defining

$$R = \frac{1}{N}\sum_{i=1}^{N} e^{i\theta_i} \tag{4.11}$$

Eq. (4.6) becomes

$$\ddot{\tilde{y}} + 2\tilde{\varepsilon}\dot{\tilde{y}} + \tilde{y} = \mathrm{Re}(R) \tag{4.12}$$

The "order parameter" *R* reflects the collective behavior of the coupled oscillator system.

In order to analyze the behavior of the system for large *N*, it is useful to take the $N \to \infty$ limit. That is, we consider a continuum of oscillators which we characterize by a distribution function $f(\theta, \tilde{\omega}, \tilde{t})$ such that $f(\theta, \tilde{\omega}, \tilde{t})d\theta d\tilde{\omega}$ is the fraction of oscillators whose phase angles lie between θ and $\theta + d\theta$ and whose

natural frequencies lie between $\tilde{\omega}$ and $\tilde{\omega}+d\tilde{\omega}$. Thus, $\iint f\, d\theta d\tilde{\omega} \equiv 1$. The natural oscillator frequencies distribution is given by $\tilde{g}(\tilde{\omega}) = \int_0^{2\pi} f\, d\theta$.

Since the number of oscillators is conserved we can write,

$$\frac{\partial f}{\partial \tilde{t}} + \frac{\partial}{\partial \theta}\left(\frac{\partial \theta}{\partial \tilde{t}} f\right) + \frac{\partial}{\partial \tilde{\omega}}\left(\frac{\partial \tilde{\omega}}{\partial \tilde{t}} f\right) = 0. \tag{4.13}$$

This equation is similar to that for particle conservation in a compressible fluid, where f plays the role of the fluid density, and $(\theta, \tilde{\omega})$ plays the role of spatial coordinates of a fluid element. For our problem, the natural frequency of an oscillator does not change with time $d\tilde{\omega}/d\tilde{t} = 0$ and $d\theta/dt$ is given by (4.7). Thus, the equations describing the $N \to \infty$ continuum limit are

$$\frac{\partial f}{\partial \tilde{t}} + \frac{\partial}{\partial \theta}\left\{\left[\tilde{\omega} - b\ddot{\tilde{y}}\cos\theta_i\right] f\right\} = 0 \tag{4.14}$$

$$R(\tilde{t}) = \int_{-\infty}^{\infty}\int_0^{2\pi} e^{i\theta} f\, d\theta d\tilde{\omega} \tag{4.15}$$

Following Ref. [18] we expand $f(\theta, \tilde{\omega}, \tilde{t})$ in a Fourier series in θ,

$$f = \frac{\tilde{g}(\tilde{\omega})}{2\pi}\left\{1 + \left[\sum_{n=1}^{\infty} f_n(\tilde{\omega}, \tilde{t}) e^{in\theta} + c.c.\right]\right\}. \tag{4.16}$$

where *c.c* stands for complex conjugate. Substituting this series expansion into (4.14) gives

$$\frac{\partial f_n}{\partial \tilde{t}} + i\, n\left\{\tilde{\omega} f_n - \frac{b}{2}\ddot{\tilde{y}}\left[f_{n+1} + f_{n-1}\right]\right\} = 0. \tag{4.17}$$

We now consider a restricted class of $f_n(\tilde{\omega}, \tilde{t})$ such that [18]

$$f_n(\tilde{\omega},\tilde{t}) = \left(\alpha(\tilde{\omega},\tilde{t})\right)^n, \tag{4.18}$$

where $\left|\alpha(\tilde{\omega},\tilde{t})\right| \le 1$ to avoid divergence of the series. Substituting this series expansion in (4.17) we get

$$\frac{\partial \alpha}{\partial \tilde{t}} + i\left\{\tilde{\omega}\alpha - \frac{b}{2}\ddot{\tilde{y}}\left[\alpha^2 + 1\right]\right\} = 0. \tag{4.19}$$

Using (4.15) and (4.18) we obtain

$$R^*(\tilde{t}) = \int_{-\infty}^{\infty} \tilde{g}(\tilde{\omega})\alpha(\tilde{\omega},\tilde{t})\, d\tilde{\omega} \tag{4.20}$$

To proceed further, we will assume walker's frequency distribution $\tilde{g}(\tilde{\omega})$ to be Lorentzian with mean $\tilde{\omega}_0$ and width $\tilde{\Delta}$,

$$\tilde{g}(\tilde{\omega}) = \frac{\tilde{\Delta}}{\pi}\frac{1}{\left(\tilde{\omega} - \tilde{\omega}_0\right)^2 + \tilde{\Delta}^2}. \tag{4.21}$$

To do the integral in (4.20) we analytically continue $\tilde{\omega}$ into the complex plane. We assume that $\alpha\left(\tilde{\omega},\tilde{t}\right)$ is analytic in $\mathrm{Im}\left(\tilde{\omega}\right) < 0$ and that $\alpha\left(\tilde{\omega},\tilde{t}\right) \to 0$ as $\mathrm{Im}\left(\tilde{\omega}\right) \to -\infty$ (see [18]). The integral in (4.20) can then be done by closing the integration path with a large semicircle in the lower half $\tilde{\omega}$ plane. The integral is given by the residue of the pole at $\tilde{\omega} = \tilde{\omega}_0 - i\tilde{\Delta}$,

$$R^*(\tilde{t}) = \alpha(\tilde{\omega}_0 - i\tilde{\Delta},\tilde{t}). \tag{4.22}$$

Thus by setting $\tilde{\omega} = \tilde{\omega}_0 - i\tilde{\Delta}$ in (4.19), we obtain

$$\frac{dR^*}{d\tilde{t}} + i\left\{(\tilde{\omega}_0 - i\tilde{\Delta})R^* - \frac{b}{2}\ddot{\tilde{y}}\left[R^{*2}(\tilde{\omega},\tilde{t}) + 1\right]\right\} = 0\,, \tag{4.23}$$

which together with (4.12) constitutes our closed low dimensional description.

Note that this description involves a single complex equation (4.23) for the order parameter $R(\tilde{t})$ characterizing the pedestrians, coupled to a second order equation (4.12) for the bridge displacement $\tilde{y}(\tilde{t})$. Thus this model exists in a four dimensional (real) state space.

4.5 Linear Analysis

In this section we examine the linear stability problem for the bridge-pedestrian system using (4.23) and (4.12).

The linearized equivalent model is given by

$$\frac{dR_r}{d\tilde{t}} + \tilde{\omega}_0 R_I + \tilde{\Delta} R_r = 0 \tag{4.24}$$

$$\frac{dR_I}{d\tilde{t}} - \tilde{\omega}_0 R_r + \tilde{\Delta} R_I = -\frac{b}{2}\ddot{\tilde{y}} \tag{4.25}$$

$$\ddot{\tilde{y}} + 2\tilde{\varepsilon}\dot{\tilde{y}} + \tilde{y} = R_r\,, \tag{4.26}$$

where $R = R_r + iR_I$

Assuming time variations proportional to $e^{s\tilde{t}}$, the previous linear system becomes

$$(s + \Delta)R_r + \tilde{\omega}_0 R_r + \tilde{\omega}_0 R_I = 0 \tag{4.27}$$

$$(s + \Delta)R_I - \tilde{\omega}_0 R_r = -\frac{b}{2}s^2\tilde{y} \tag{4.28}$$

$$(s^2 + 2\tilde{\varepsilon}s + 1)\tilde{y} = R_r \tag{4.29}$$

Nontrivial solution for R and $\tilde{y}$ occur when *s* satisfies the characteristic equation

$$\left[(s+\Delta)^2+\tilde{\omega}_0{}^2\right]\left(s^2+2\varepsilon s+1\right)=\frac{b}{2}s^2\tilde{\omega}_0 \tag{4.30}$$

To obtain the critical value of *b* (denoted b_c) at the onset of instability, we set $s=i(\tilde{\omega}_0+\delta_I)$ and $b=b_c$ in (4.30). Furthermore, noting that for the Millennium Bridge the dimensionless quantities $\tilde{\varepsilon}$, $|\tilde{\omega}_0-1|$, $\tilde{\Delta}$ are small, we introduce the ordering,

$$|\tilde{\omega}_0-1|\sim\tilde{\varepsilon}\sim\tilde{\Delta}\sim\delta_I\sim\sqrt{b_c}<<1. \tag{4.31}$$

Utilizing this in (4.30) and expanding to lowest order in the small quantities, the real and imaginary parts of (4.30) give the following equations for b_c and δ_I,

$$\tilde{\Delta}\left(1-\tilde{\omega}_0-\delta_I\right)=\tilde{\varepsilon}\,\delta_I \tag{4.32}$$

$$\delta_I\left(1-\tilde{\omega}_0+\delta_I\right)+\tilde{\Delta}\,\tilde{\varepsilon}=b_c/8 \tag{4.33}$$

Solving (4.32) for δ_I and substituting into (4.33), we obtain the critical value b_c, such that for $b>b_c$ there is instability,

$$b_c=8\tilde{\Delta}\tilde{\varepsilon}\left[1+\left(\frac{\tilde{\omega}_0-1}{\tilde{\Delta}+\tilde{\varepsilon}}\right)^2\right] \tag{4.34}$$

For the worst case, $\tilde{\omega}_0=1$, the critical *b* value is given by

$$b_c=8\tilde{\Delta}\tilde{\varepsilon} \tag{4.35}$$

Figure 4.1 shows the relationship between b_c and $\tilde{\omega}_0$.

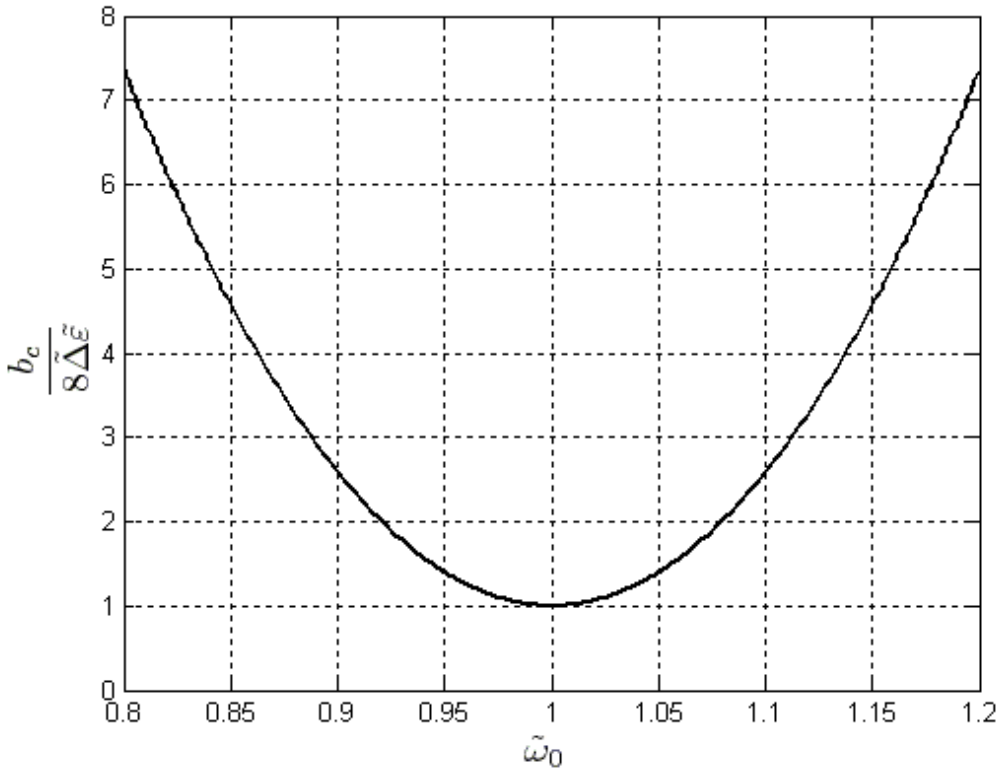

Figure 4.1: Relationship between walker's average frequency $\tilde{\omega}_0$ and b_c

For the case $\tilde{\omega}_0 = 1$, Eq. (4.30) evaluated to lowest order in the small quantities previously given, yields

$$\gamma^2 + \left(\tilde{\Delta} + \tilde{\varepsilon}\right)\gamma + \tilde{\Delta}\tilde{\varepsilon} = b/8 \tag{4.36}$$

where we have defined $s = i + \gamma$. Equation (4.36) yields

$$\gamma = \frac{1}{2}\left[\sqrt{\left(\tilde{\Delta} + \tilde{\varepsilon}\right)^2 + \frac{1}{2}\left(b - b_c\right)} - \left(\tilde{\Delta} + \tilde{\varepsilon}\right)\right] \tag{4.37}$$

which is positive, corresponding to instability, for $b > b_c = 8\tilde{\Delta}\tilde{\varepsilon}$, and negative, corresponding to exponential damping, for $b < b_c$.

4.6 Nonlinear Steady State Solution

In this section we study the steady state behavior of the system model for the worst case $\tilde{\omega}_0 = 1$, i.e., when the walkers' frequency matches the bridge eigenfrequency. In the steady state case, the oscillation observed on the opening day can be modeled as

$$y(\tilde{t}) = A\cos(\tilde{t}). \tag{4.38}$$

Taking the order parameter in the steady state to be

$$R(\tilde{t}) \cong iR_\infty e^{i\tilde{t}} \tag{4.39}$$

where R_∞ is real , and substituting with (4.39) in (4.23) we get

$$-R_\infty e^{-i\tilde{t}} + i\left[\left(1-i\tilde{\Delta}\right)\left(-iR_\infty e^{-i\tilde{t}}\right)+\frac{b}{4}A\left(e^{i\tilde{t}}+e^{-i\tilde{t}}\right)\left(-R_\infty^2 e^{-2i\tilde{t}}+1\right)\right]=0 \tag{4.40}$$

Which consists of terms varying as $e^{-i\tilde{t}}$, $e^{i\tilde{t}}$, $e^{-3i\tilde{t}}$. Consistent with our approximation (4.31) we ignore the components varying as $e^{i\tilde{t}}$ and $e^{-3i\tilde{t}}$. Thus setting the coefficient of the $e^{-i\tilde{t}}$ term to zero, we obtain,

$$bA = \frac{4\Delta R_\infty}{1-R_\infty^2} \quad . \tag{4.41}$$

Substituting (4.39) in (4.12), we get

$$A = \frac{R_\infty}{2\varepsilon} \quad . \tag{4.42}$$

Equations (4.41), (4.42), and $b_c = 8\Delta\varepsilon$, yield

$$R_\infty = \sqrt{1-\frac{b_c}{b}} \tag{4.43}$$

Figure 4.2 shows the relationship between the steady state amplitude *A* and the *b* value. We will subsequently verify the accuracy of the approximations used above by comparing Eq. (4.41) with numerical solutions of the full system.

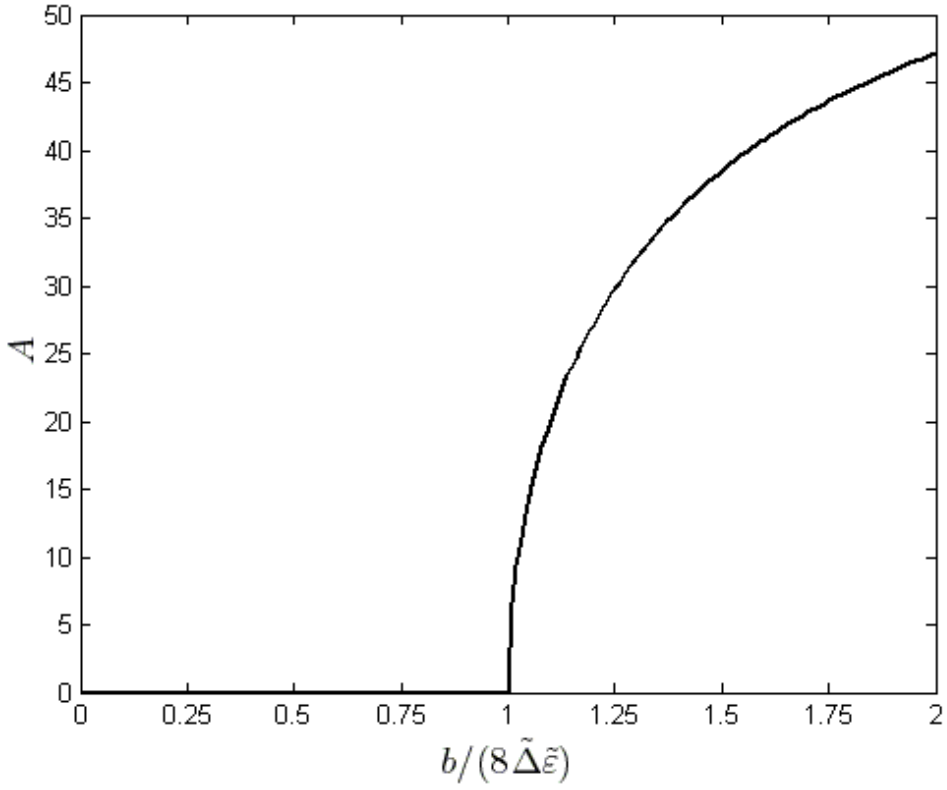

Figure 4.2: Steady state amplitude *A* versus *b* value.

Chapter 5: Numerical Simulations

In this chapter we will conduct several simulations to verify the results in chapter 4, as well as to obtain additional results and to compare our results with Arup's experiments.

5.1 Simulation Program

We wrote a program to solve the bridge reduced ODE system derived in chapter 4. The Runge-Kutta method is implemented to the forth degree to solve the ODE system.

5.2 Simulation Parameters

The following parameters are used in all the simulations in this chapter except when explicitly mentioned.

Table 5.1: Simulation parameters used throughout the chapter.

	Symbol	Value	Reference
Bridge model	M	$113\text{x}10^3\ Kg$	[4]
	$\tilde{\varepsilon}$	0.0075	[4]
	τ	1.9 sec	[3]
	g_0	$0.3\ m/s^2$	[3]
	Ω	$2\pi/s$	[4]
Pedestrian model	f_0	$25\ N$	[21]
	$\tilde{\sigma}$	0.09	[21]
	$\tilde{\Delta}$	0.072	Assumed
Initial conditions	$\tilde{y}(0)$	10^{-3}	Arbitrary
	$\dot{\tilde{y}}(0)$	0	Arbitrary

5.3 Time Evolution of the System for Constant Coupling Coefficient b

In this section we will examine the system time evolution when the coupling coefficient *b* is not varied with time. This is the case of a fixed number of walkers.

Two cases will be examined, one with $b > b_c$, and one with $b < b_c$. In each case, we will solve the ODE system, Eqs. (4.23) and (4.12), and plot the normalized bridge displacement $\tilde{y}$ versus time and the magnitude of the order parameter $|R|$ versus time.

5.3.1 Case I: $b > b_c$

In this case we will use $b = 1.25 b_c$. Figure 5.1 shows the time evolution of the bridge normalize oscillation amplitude. Starting from a small value of $\tilde{y}$, the bridge started to build up oscillation until it reached the steady state with peak oscillation amplitude of 2.25 (dimensionless).

Figure 5.2 is a magnification of a part of Fig. 5.1. It shows the initial approximate exponential growth of the bridge oscillation.

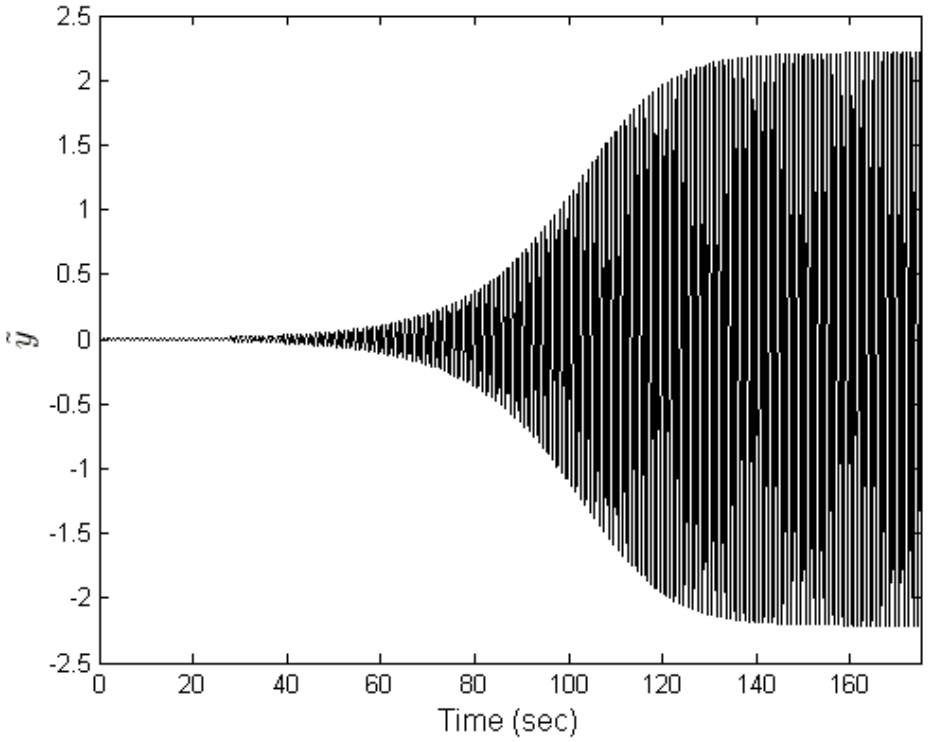

Fig. 5.1: Normalized amplitude versus time for the case $b > b_c$. $b = 1.25 b_c$ is used.

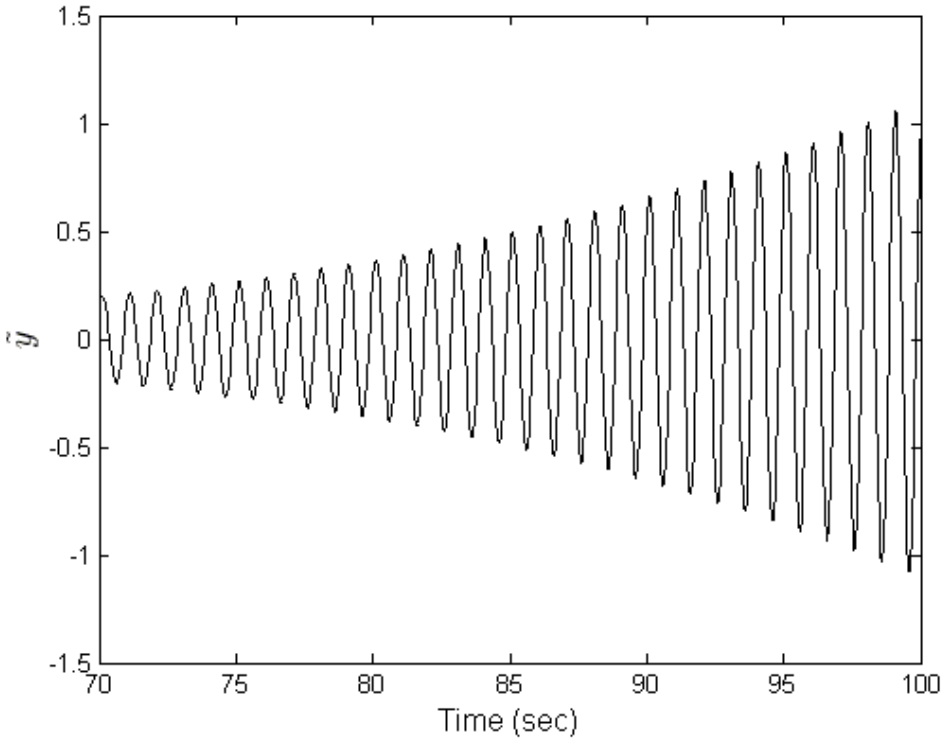

Figure 5.2: Magnification of a part of Fig. 5.1, showing the bridge oscillation buildup.

Figure 5.3 shows a semilog plot of the time evolution of $|R|$. We see that the pedestrian forcing started increases exponentially exponential rate until it reached a steady state value of $R_\infty = 0.44$.

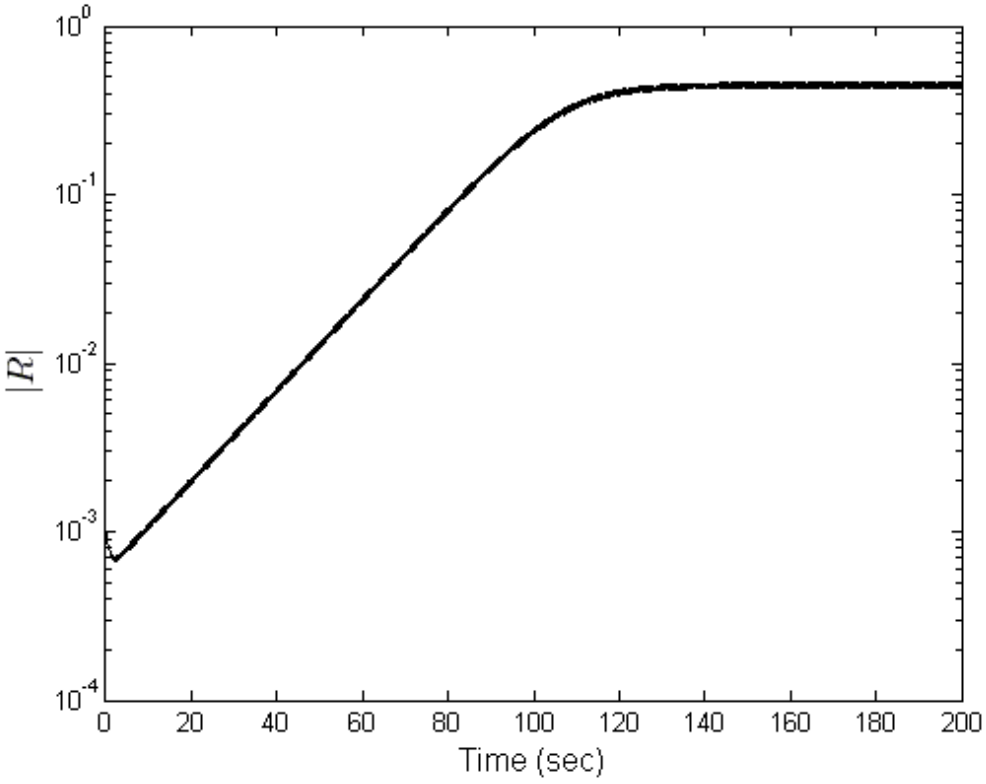

Figure 5.3: Order parameter $|R|$ versus time for the case $b > b_c$. $b = 1.25 b_c$ is used

5.3.2 Case II: $b < b_c$

To illustrate this case, we used $b = 0.75 b_c$. Figure 5.4 shows the time evolution of the normalized bridge oscillation amplitude $\tilde{y}$. Starting from a small *y*, the bridge oscillation damps exponentially toward zero.

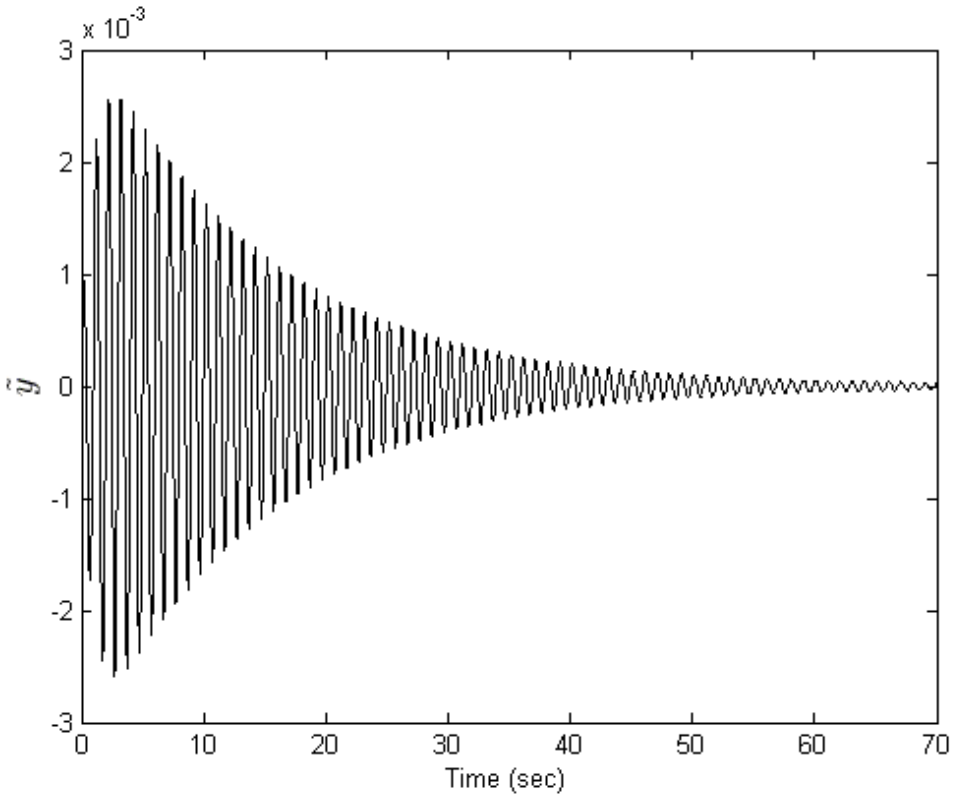

Figure 5.4: Normalized amplitude versus time for the case $b < b_c$. $b = 0.75 b_c$ and $|R(0)| = 10^{-3}$ are used.

Figure 5.5 shows the time evolution of $|R|$. The pedestrian force decreases exponentially with time.

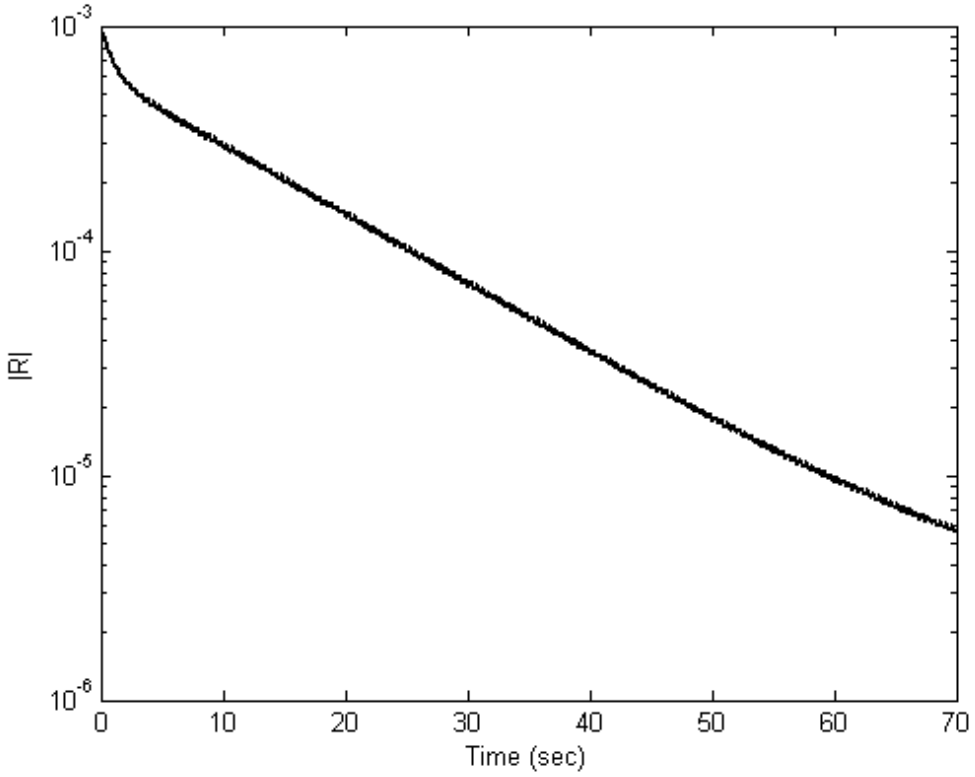

Figure 5.5 Order parameter $|R|$ versus time for the case $b < b_c$. $b = 0.75 b_c$ and $|R(0)| = 10^{-3}$ are used

5.4 Validation of the Non-Linear Model

In this section we will compare our analytical results, Eqs. (4.34), (4.35), (4.37), (4.42), and (4.43) from section 4.6, with the solution of the ODE system.

In the following simulations we scanned all the *b* values from $b_{start} = \tilde{\Lambda}\tilde{\varepsilon}$ to $b_{end} = 16\tilde{\Lambda}\tilde{\varepsilon}$ with step size $0.1\tilde{\Lambda}\tilde{\varepsilon}$.

Figure 5.6 shows the normalized amplitude *A* versus the *b* value. A sudden change in the normalized amplitude can be notice at $b = 8\tilde{\Lambda}\tilde{\varepsilon}$. Before this value, the bridge is considered to be stable and after it, the bridge started to oscillate. We note a

small discrepancy between the theory and the numerical solution (the x's). This is probably due to the approximations in Eq. (4.41).

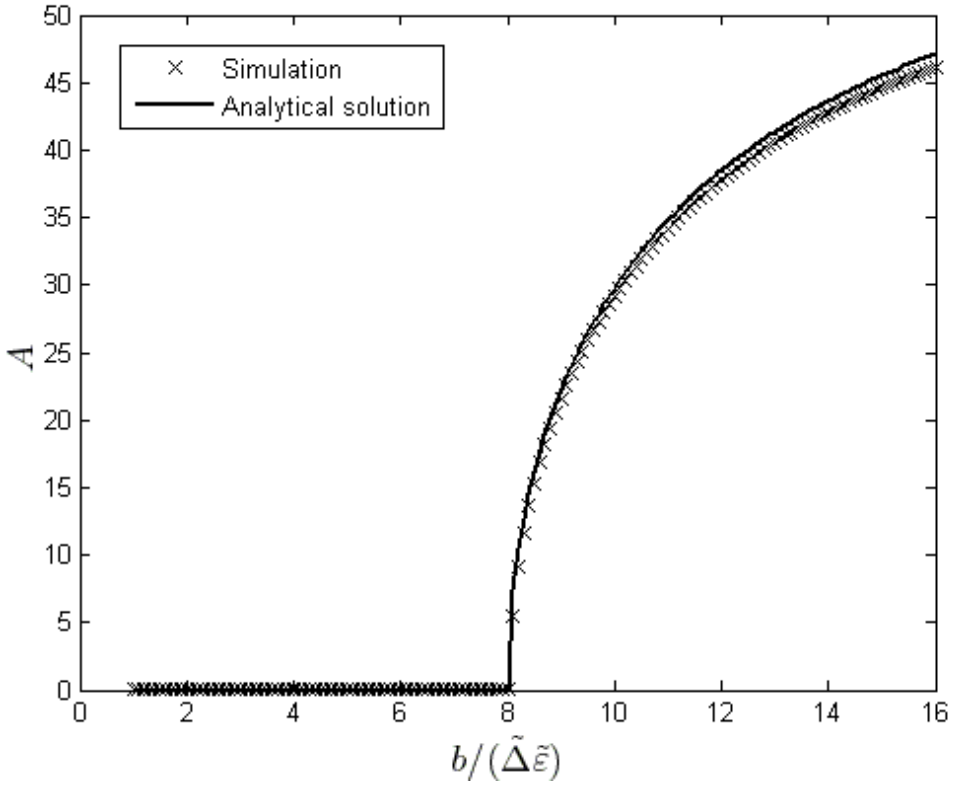

Fig 5.6: Effect of varying the coupling coefficient *b* on the normalized steady state oscillation amplitude (*A*). Solid line is the analytical solution and the (x-marker) is the simulation.

Figure 5.7 shows R_∞ verses the coupling parameter *b*. The synchronization can also be noticed at $b = 8\tilde{\Delta}\,\tilde{\varepsilon}$.

Figure 5.6 and 5.7 verifies the accuracy of Eqs. (4.42) and (4.43) the non-linear steady state amplitude *A* and the steady state walker forcing R_∞.

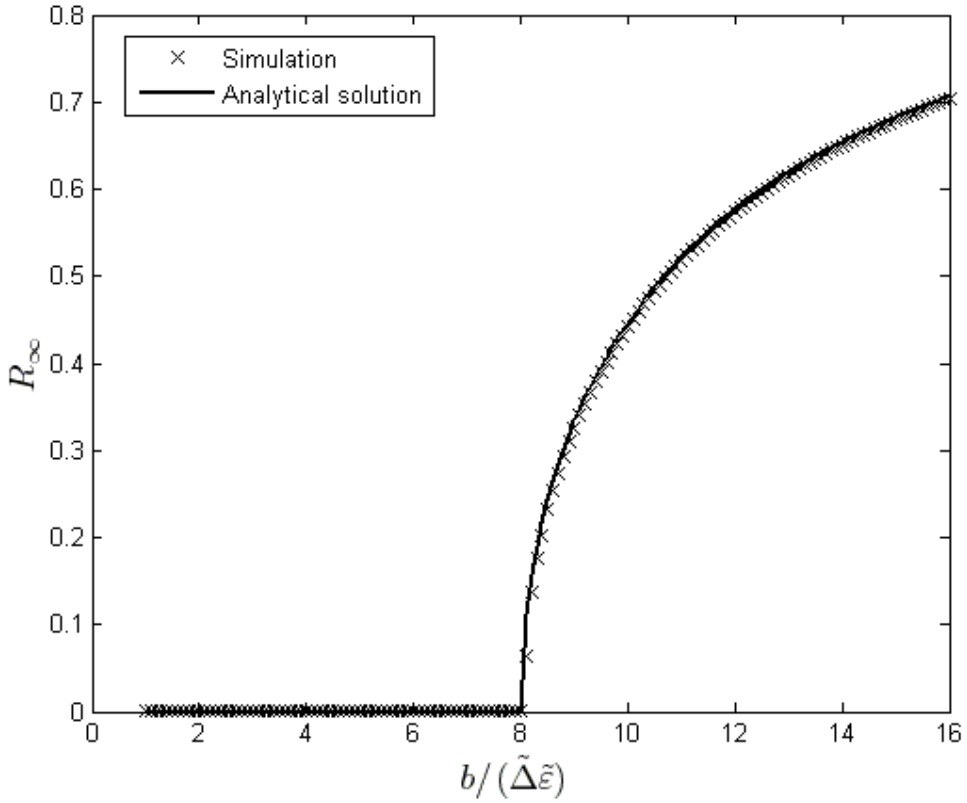

Fig 5.7: Effect of varying the coupling parameter *b* on the order parameter steady state R_∞. Solid line is the analytical solution and the (x-marker) is the simulation.

In the third simulation we want to verify the growth rate equation as well as the critical coupling coefficient b_c value. Because we are interested in the stability condition, we scanned the *b* values around b_c and not all the b_c range as we done in the previous simulations.

Figure 5.8 shows the growth rate γ verses the coupling coefficient *b*. We can see how the simulation (x's) matches the analytical solution [Eq. (4.37)] especially for the value of b_c. The zero crossing occurs at $b_c = 8.02\tilde{\Delta}\tilde{\varepsilon}$ which matches the analytical value $b_c = 8\tilde{\Delta}\tilde{\varepsilon}$.

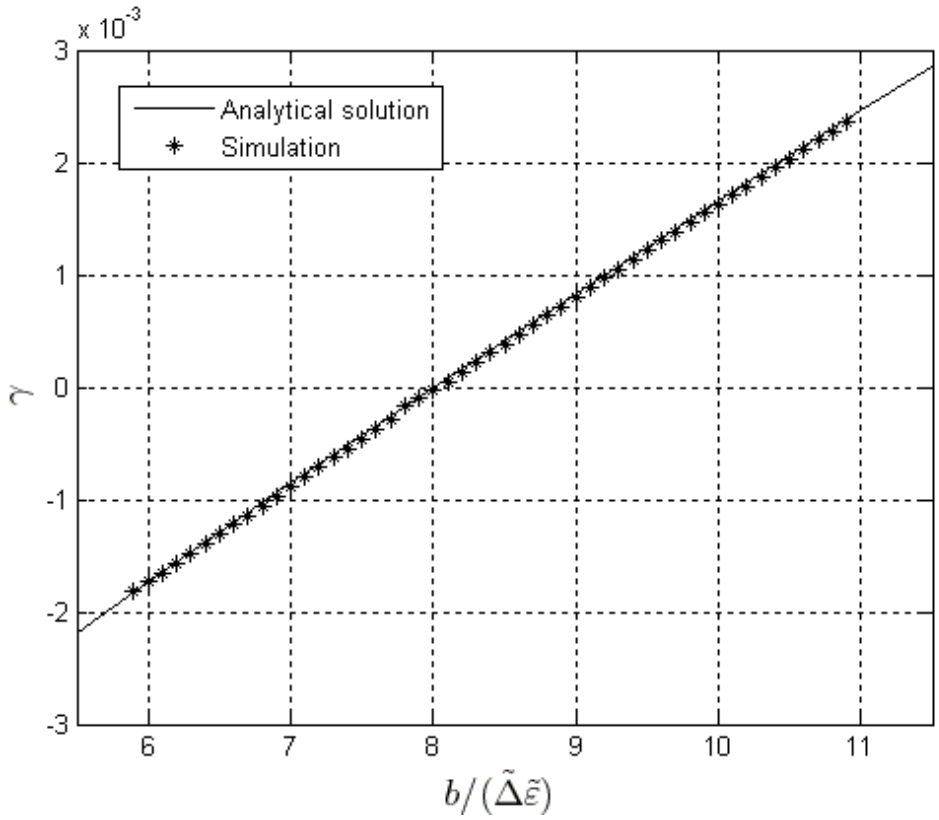

Fig 5.8: Effect of varying the coupling coefficient *b* on the growth rate of $|R|$. Solid line is the analytical solution [Eq. (4.37)] and the (x-marker) is the simulation.

5.5 Effect of Different Mean Walker Frequency

In the previous sections, we assumed that the walker's frequency matches the bridge eigenfrequency, i.e. $\tilde{\omega}_0 = 1$.

Now we investigate what happens if $\tilde{\omega}_0 \neq 1$. In this section we will verify the result in section 4.5, using simulations.

The program starts by setting $\tilde{\omega}_0 \in [0.8,1.2]$. For a given $\tilde{\omega}_0$ value, we change *b* from $b_{start} = \tilde{\Delta}\tilde{\varepsilon}$ to $b_{end} = 16\tilde{\Delta}\tilde{\varepsilon}$ with step $0.1\tilde{\Delta}\tilde{\varepsilon}$. For each *b* value the corresponding growth rate is recorded. After we finish scanning all the *b* values, the

growth rate data is then fitted to a linear model and the corresponding b_c is determined as in section 5.5. This procedure is repeated for each $\tilde{\omega}_0 \in [0.8,1.2]$ with step size 0.5.

Figure 5.9 shows the results of the simulation and the analytical solution given by (4.34).

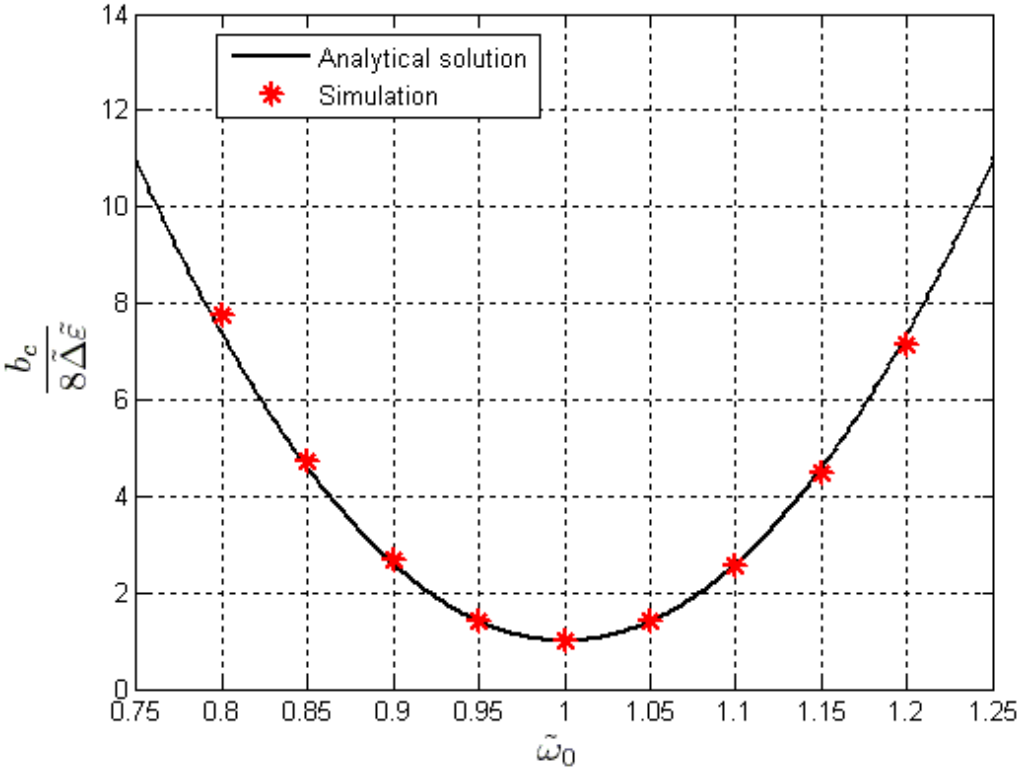

Figure 5.9: Effect of varying the walker's mean frequency $\tilde{\omega}_0$ on the critical coupling value (which corresponds to the critical number of walkers)

The match between the analytical solution and the simulation shows the accuracy of the approximations used in obtaining the analytical result.

5.6 Time Variation of the Number of Walkers

Following the discovery of the walker-induced wobble of the Millennium Bridge, the bridge builder company (Arup) conducted a controlled test as discussed in chapter 2. We now wish to adapt our formulation to simulate those tests. Since we regard the newly introduced walkers to initially be randomly distributed in phase at the time of introduction, we will allow for a different Lorentzian distribution function for each group of walkers. Adapting our previous formulation to this consideration, we have in place of (3.1)

$$M\ddot{y} + 2M\varepsilon\dot{y} + M\Omega^2 y = f_0 \sum_{j=1}^{J(t)} N_j \,\mathrm{Re}\left[R_j(t)\right], \tag{5.1}$$

where N_j walkers are introduced onto the bridge at the time t_j, the number $J(t)$ of groups on the bridge at time *t* is defined by

$$t_{J+1} > t \geq t_J \ , \tag{5.2}$$

and the complex quantity $R_j(t)$ characterizes the distribution of walkers in group *j*. for $t \geq t_j$, $R_j(t)$ satisfies Eq. (4.23) with the initial condition,

$$R_j(t_j) = 0, \tag{5.3}$$

corresponding to the walker phases being randomly distributed at the time when they first enter the bridge. Thus, by virtue of their different times of entry, Eq. (5.3) implies a different distribution of oscillator phases for each group.

In this simulation we simulated a total number of 200 walkers divided on 20 groups; i.e. 10 walkers/group. We used equal time intervals of 1 minute between each group and its predecessor.

Figure 5.10 show three plots. The first plot is the number of walkers versus time. The second plot is the maximum amplitude of the bridge lateral oscillation versus time. The third plot is the system order parameter defined as

$$R = \frac{1}{20}\left|\sum_{j=1}^{J(t)} R_j\right| \tag{5.4}$$

versus time (note: 20 is the number of groups).

These plots show the same general behavior as that in Fig. 2.2 for the Arup experiment; i.e., there is little oscillation until the pedestrian number build up, and then the oscillation rapidly increases.

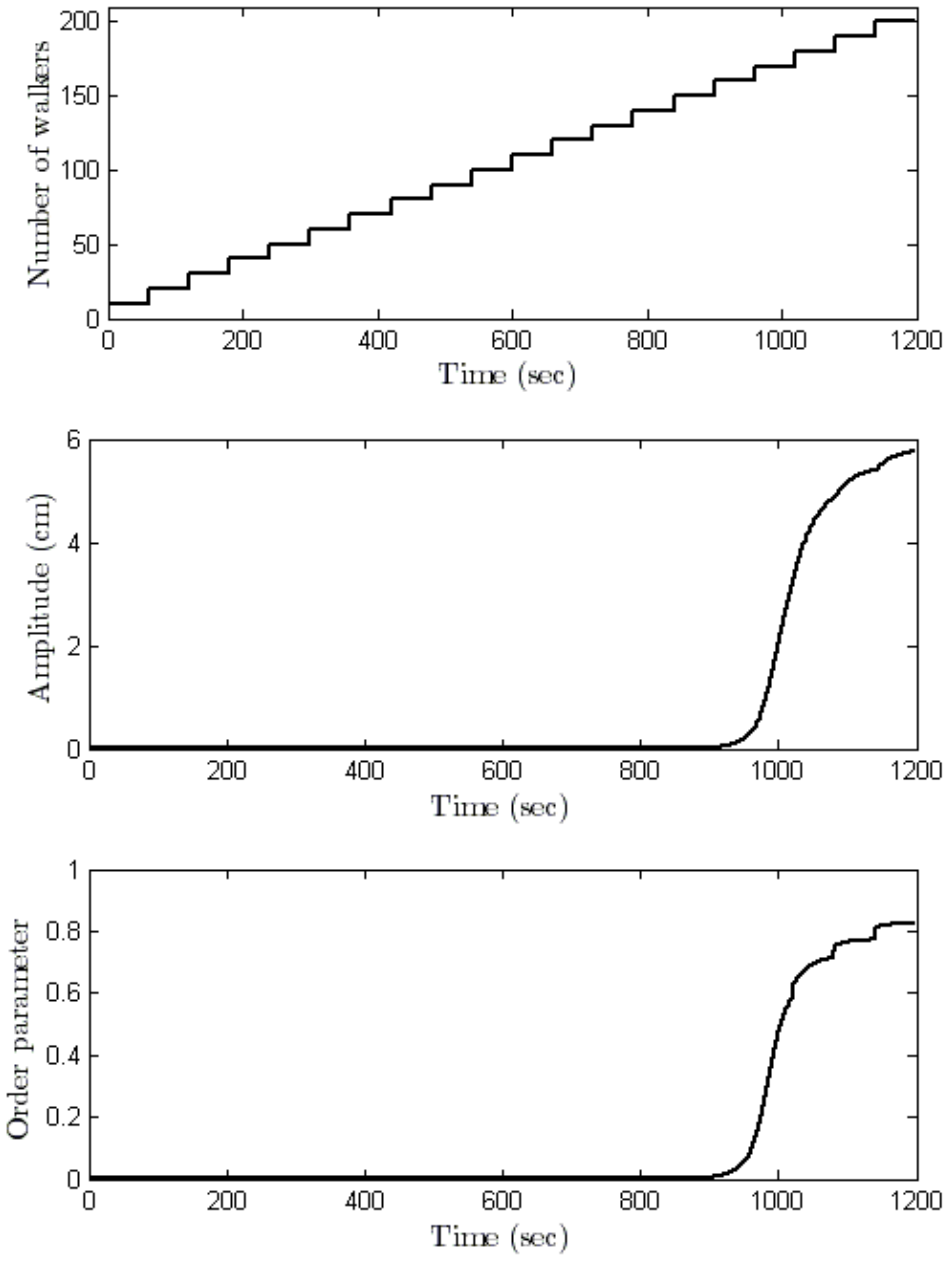

Figure 5.10: Effect of adding more walkers to the bridge as a function of time. The first plot is the number of walkers versus time. The second is the maximum oscillation amplitude versus time. The third is the system order parameter versus time.

Chapter 6: Conclusions

The Eckhardt *et al.* model addresses the synchronization mechanism of individual walkers and the resulting global response of the bridge-pedestrian system. Using the method in [18], we were successful at reducing the complexity of this model from ($N+2$) state space dimensionals to just 4 for the case of fixed number of walkers. The same method was also used to simplify the treatment of different groups of walkers entering the bridge at different times.

Numerical simulations, in chapter 5, agreed with analytical solutions presented in chapter 4. The simulation time of the low dimensional order system was much less than that for the original Eckhardt *et al.* model.

More generally, our work serves as an interesting example of the potential for low dimensional macroscopic behavior in systems consisting of many coupled oscillators.

Bibliography

[1] H. Bachmann and W. Ammann, "Vibrations in Structures Induced by Man and Machines", *Structural Engineering Document 3e*, International Association for Bridge and Structural Engineering (IABSE), Ch. 2: Man-Induced Vibrations, and Appendix A: Case Reports, 1987.

[2] A. Belli, P. Bui, A. Berger, A. Geyssant, and J. Lacour. "A treadmill ergometer for three-dimensional ground reaction forces measurement during walking," *J Biomech*, vol. 34, pp. 105-112, 2001.

[3] B. Eckhardt, E. Ott, S. H. Strogatz, D. Abrams, A. McRobie. "Modeling walker synchronization on the Millennium Bridge," *Phys. Rev. E,* vol. 75, 021110, 2007.

[4] P. Dallard, A. J. Fitzpatrick, A. Flint, S. Le Bourva, A. Low, R. M. R. Smith, and M. Willford. "The London Millennium footbridge," *The Structural Engineer*, 79:22, pp.17-35, Nov 2001.

[5] P. Dallard, A. J. Fitzpatrick, A. Flint, A. Low, R. M. R. Smith, M. Willford, and M. Roche. "London Millennium Bridge: Pedestrian-induced lateral vibration," *Journal of Bridge Engineering*, 6:6, pp. 412-417, Nov/Dec 2001.

[6] A. Fitzpatrick, P. Dallard, S. Le Bourva, A. Low, R. M. R. Smith, and M. Willford. "Linking London: The Millennium Bridge," *Royal Academy of Engineering*, pp. 1-28, Jun 2001.

[7] Y. Fujino, B. M. Pacheco, S. Nakamura, and P. Warnitchai. "Synchronization of human walking observed during lateral vibration of a congested pedestrian bridge," *Earthquake Engineering and Structural Dynamics*, 22, pp. 741-758, 1993.

[8] R. Haubler, R. Bartussek, and P. Hanggi, in Applied Nonlinear Dynamics and Stochastic Systems Near the Millennium, edited by J. B. Kadtke and A. Bulsara, AIP Conf. Proc. No. 411 (AIP, New York, 1997) pp. 243–248.

[9] Z. Kiss, Y. Zhai and J. L. Hudson, "Emerging Coherence in a Population of Chemical Oscillators," *Science*, 296, pp. 1676, 2005.

[10] Y. Kuramoto, in International Symposium on Mathematical Problems in Theoretical Physics, Lecture Notes in Physics, Vol. 39, edited by H. Araki (Springer-Verlag, Berlin, 1975); Chemical Oscillations, Waves and Turbulence (Springer, 1984).

[11] Y. Matsumoto, S. Sato, T. Nishioka, H. Shiojiri. “A study on design of pedestrian over-bridges,” *Transactions of JSCE*, 4, pp. 50–51, 1972.

[12] Y. Matsumoto, T. Nishioka, H. Shiojiri, K. Matsuzaki. “Dynamic design of footbridges”, *IABSE Proceedings*, 17:78, pp. 1-15, 1978.

[13] A. McRobie and G. Morgenthal, “Full-scale section model tests on human-structure lock-in”, Proc. Int. Conf. *footbridge 2002*, Paris, 2002.

[14] A. McRobie and G. Morgenthal, “Risk Management for Pedestrian-Induced Dynamics of Footbridges”, Proc. Int. Conf. *footbridge 2002*, Paris, 2002.

[15] S. Nakamura. “Model for lateral excitation of footbridges by synchronous walking,” *Journal of Structural Engineering*, 130, pp. 32-37, Jan 2004.

[16] D. Newland. “Vibration of the London Millenium Footbridge: cause and cure,*” Int. J. of Acoustics and Vibration*, 8, 1, 9-14, 2003

[17] E. Ott, *Chaos in Dynamical Systems*, 2nd ed., Cambridge University Press, Cambridge, 1998, pp. 236–244.

[18] E. Ott and Thomas M. Antonsen. “Low Dimensional Behavior of Large Systems of Globally Coupled Oscillators,” arXiv:0806.0004v1, *Chaos* (to be published, Sept. 2008).

[19] T. M. Roberts. “Synchronised pedestrian excitation of footbridges,” *Bridge Engineering*, 156, pp. 155-160, Dec 2003.

[20] S. Yamaguchi, *et al.*, “Synchronization of Cellular Clocks in the Suprachiasmatic Nucleus,” *Science*, 302, pp. 1408, 2002.

[21] S. Zivanovic, A. Pavic, and P. Reynolds. “Vibration Serviceability of Footbridges under Human-Induced Excitation: A Literature Review”. *Journal of Sound and Vibration*, vol. 279, No 1-2, pp. 1-74, 2005.